The Quadruple Gravitational Lens PG1115+080: Time Delays and Models

Paul L. Schechter[1], Charles D. Bailyn[2], Robert Barr[3], Richard Barvainis[4], Christopher M. Becker[1], Gary M. Bernstein[5], John P. Blakeslee[1], Schelte J. Bus[6], Alan Dressler[7], Emilio E. Falco[8], Robert A. Fesen[9], Phillipe Fischer[5,10], Karl Gebhardt[5], Dianne Harmer[11], Jacqueline N. Hewitt[1], Jens Hjorth[12], Todd Hurt[13], Andreas O. Jaunsen[14], Mario Mateo[5], Doerte Mehlert[15], Douglas O. Richstone[5], Linda S. Sparke[16], John R. Thorstensen[9], John L. Tonry[1], Gary Wegner[9], Daryl W. Willmarth [11] and Guy Worthey[5,10]

ABSTRACT

Optical photometry is presented for the quadruple gravitational lens PG1115+080. A preliminary reduction of data taken from November 1995 to June 1996 gives component “C” leading component “B” by 23.7 ± 3.4 days and

---

[1] Department of Physics, Massachusetts Institute of Technology, Cambridge MA 02138

[2] Department of Astronomy, Yale University, New Haven CT 06520-8101

[3] Michigan-Dartmouth-MIT Observatory HC 04 P.O. Box 7520, Tucson AZ 85634

[4] MIT Haystack Observatory, Westford MA 01886

[5] Department of Astronomy, University of Michigan, Ann Arbor MI 48109

[6] Department of Earth Atmospheric and Planetary Sciences, Massachusetts Institute of Technology, Cambridge MA 02139

[7] Carnegie Observatories, Carnegie Institution of Washington, 813 Santa Barbara Street, Pasadena CA 91101

[8] Harvard-Smithsonian Center for Astrophysics, 60 Garden Street, Cambridge MA 02138

[9] Department of Physics and Astronomy, Dartmouth College, Hanover NH 03755-3528

[10] Hubble Fellow

[11] National Optical Astronomy Observatories, P.O. Box 26732, Tucson AZ 85726

[12] Institute of Astronomy, Madingly Road, Cambridge CB3 0HA, England

[13] Department of Physics, University of California, Santa Barbara CA 93106

[14] Nordic Optical Telescope, E-38700 Canarias, Spain

[15] Universitaetssternwarte Muenchen, D-81679 Muenchen, Germany

[16] Washburn Observatory, University of Wisconsin, Madison WI 53706

components “A1” and “A2” by 9.4 days. A range of models has been fit to the image positions, none of which gives an adequate fit. The best fitting and most physically plausible of these, taking the lensing galaxy and the associated group of galaxies to be singular isothermal spheres, gives a Hubble constant of 42 km/s/Mpc for $\Omega = 1$, with an observational uncertainty of 14%, as computed from the $B - C$ time delay measurement. Taking the lensing galaxy to have an approximately E5 isothermal mass distribution yields $H_0 = 64$ km/sec/Mpc while taking the galaxy to be a point mass gives $H_0 = 84$ km/sec/Mpc. The former gives a particularly bad fit to the position of the lensing galaxy, while the latter is inconsistent with measurements of nearby galaxy rotation curves. Constraints on these and other possible models are expected to improve with planned HST observations.

Subject headings: cosmology: distance scale, gravitational lensing — quasars, photometry

1. Introduction

Among the most promising applications of gravitational lenses is their use in determining cosmological distances (Refsdal 1964; Blandford and Narayan 1992). One measures fluxes for the components of a multiply imaged variable object as a function of time and determines the differential time delays. Though straightforward in principle, both the measurement of time delays and their interpretation has proven difficult in practice. Only recently have measurements for 0957+561 (Haarsma *et al.* 1996a,b and Kundić *et al.* 1996 confirming the result of Schild and Cholfin 1986) and their interpretation (e.g. Grogin and Narayan 1996) begun to converge.

The quadruply imaged $z = 1.722$ quasar PG1115+080 (Weymann *et al.* 1980; see Figure 1) has many properties which recommend it as a candidate for time delay measurements (Schechter 1996). But while PG1115+080 is known to vary (Vanderriest *et al.* 1986), and though the flux ratios of the components appear to have varied (Schechter 1996), as yet no time delay has been reported. In the following sections we report measurement of multiple time delays from a preliminary reduction of data taken from November 1995 to June 1996.

2. Observations and Reduction

Direct V filter CCD exposures were taken with the Hiltner 2.4-m telescope, the WIYN 3.5-m telescope, the NOT 2.5-m telescope and the Dupont 2.5-m telescope, always in multiples of at least three exposures, typically 6 minutes each. Frames were bias subtracted and flatfielded and charged particle events were identified and flagged. Six bright stars were used to obtain the image scale and rotation.

Photometry was carried out using methods nearly identical to those used by Schechter and Moore (1993) for the lens MG0414+0534. In the present case positions for the lensing galaxy and the four quasar images relative to each other were established from V exposures taken in 1994 with $0\farcs75$ seeing, as were the shape parameters and the galaxy flux. The galaxy shape was convolved with the seeing appropriate to each image. Fixing the relative positions and the galaxy shape and flux leaves six parameters to be determined from each frame – the four quasar fluxes and the overall position of the system.

Quasar fluxes were obtained relative to the nearby star designated "C" by Vanderriest *et al.* (1986), which was used as an empirical point spread function (PSF) template. Fluxes for other nearby stars relative to star "C" were also measured. No attempt was made to correct for color dependent airmass terms.

Fluxes were summed for the two brightest components, $A1$ and $A2$, which are separated by only $0\farcs48$. Little is lost because the time delay between $A1$ and $A2$ is expected to be hours. Fluxes for each multiplet of exposures were converted to relative magnitudes and averaged together, and an rms scatter computed. The median scatters for components $A1 + A2$, C and B were, respectively, 4, 7 and 13 millimagnitudes. These were roughly 50% bigger than the formal errors in the fits.

The average magnitudes for the quasar components and for star "B" are plotted[17] in Figure 2. They include 30 nights of data from MDM Observatory and 2 from the NOT. Multiple entries on the same night indicate exposures taken with slightly different "V" filters.

Fifteen nights of data taken with the WIYN 3.5-m telescope were also reduced but are not included. The seeing at the WIYN and the intranight consistency of these data were superb. However the night-to-night consistency was poor, and it has not proven possible to bring the MDM data and the WIYN data into accord. We expect that by allowing for variation in the PSF across the chip we will ultimately be able to combine the two data

---

[17] These data can be found in tabular form at http://arcturus.mit.edu/~ schech/pg1115.html

sets.

3. Photometric Results

In the light curves for components $A1 + A2$, C and B shown in Figure 2, the errors in the means, as computed from the intranight scatter, are not much larger than the symbols. The night-to-night agreement is considerably worse; likewise the agreement of the shifted lightcurves is much worse than expected from the intranight scatter. On at least some nights the fluctuations, and those of star "B", appear to be correlated (e.g. JD 24450088). It seems likely that these are due to errors in the adopted PSF. Therefore in plotting the quasar components in Figures 2 and 3, and in estimating time delays, we have subtracted one half the magnitude of star "B" (taken with respect to star "C") from our magnitudes for the quasar components (also taken with respect to star "C"). This gives equal weight to stars "B" and "C" as photometric references.

The amplitude for components $A1 + A2$ appears somewhat smaller than that for C or B, but this is not unexpected. Witt, Mao and Schechter (1995) find that unresolved components suffer rms fluctuations of 0.6 mag due to microlensing in quadruply imaged systems. If the time variable core is unresolved by the microlenses, while most of the flux arises from a larger, resolved region, one expects different fractional flux changes in the different components.

4. Time Delay

We have computed time delays and flux ratios for the $(A1 + A2) - C$ and $B - C$ pairs, using the method of Press, Rybicki, and Hewitt (1992), but generalized so that the four parameters are fit to the three light curves simultaneously. Since the errors derived from the intranight scatters are clearly too small, we have added to these, in quadrature, additional errors of 4, 7, and 10 millimag for components $A1 + A2, C$, and B respectively. The present analysis incorporates the implicit assumptions a) that the errors are uncorrelated and b) that the fractional flux variations are the same for each component.

Under these assumptions, we find component C leading component $A1 + A2$ by 9.4 days, and component C leading component B by 23.7 days. The best-fit $C/(A1 + A2)$ flux ratio is 0.153 and the best-fit B/C flux ratio is 0.634. It follows that component $A1 + A2$ leads B by 14.3 days and that the $B/(A1 + A2)$ flux ratio is 0.097. Figure 3 shows lightcurves for components B and C, with the latter delayed.

A plot of the χ^2 statistic for the $(A1 + A2) - C$ and $B - C$ delays shows a clean elliptical minimum, indicating an error for the $B - C$ delay which is 10% larger than for $(A1 + A2) - C$, with a positive correlation coefficient of approximately 0.5. This implies that $B - (A1 + A2)$ delay is correlated with the $B - C$ delay and anticorrelated with the $(A1 + A2) - C$ delay at roughly the same level. The minimum value of χ^2 was 146, with $\nu = 86$ degrees of freedom. Scaling errors to give $\chi^2/\nu = 1$ gives errors of roughly ~ 0.8 days.

Monte Carlo simulations of the B and C components spanning a broad range of delays and fitting only for the $B - C$ delay give an rms scatter of ±3.4 days for the time delay, with only a weak dependence on delay length. These are considerably larger than those obtained from the χ^2 surface, for reasons discussed by Press, Rybicki and Hewitt (1992). Had we simulated all three components and fit for the delays simultaneously the scatter might have been smaller. For the present we adopt ±3.4 days as a best estimate for all of the delays.

5. Models, Distance and Hubble's Constant

We have fit four models for the gravitational potential to the HST positions (but not the fluxes) of Kristian *et al.* (1993) for the purpose of transforming our time delay into a distance. All but one take the lensing galaxy to have a logarithmic 3-D potential, which would produce flat rotation curve for circular orbits. Model PMXS is a point mass with external shear. Model ISXS is an isothermal sphere with external shear. Model ISEP is an isothermal elliptical potential (Blandford and Kochanek 1987). The ISIS model, adopted by Hogg and Blandford (1995) in modelling B1422+231, uses a second isothermal sphere to provide shear. We identify this second isothermal with the z=0.304 group of galaxies (Young *et al.* 1981; Henry and Heasley 1986) at approximately the same redshift as measured for the lensing galaxy by Angonin-Willaime *et al.* (1993).

The dimensionless 2-D "effective lensing potentials" ψ are given by

$$\psi_{PMXS}(\vec{\theta}) = b^2 \ln r + \frac{\gamma}{2} r^2 \cos 2(\theta - \theta_\gamma) \quad , \tag{1a}$$

$$\psi_{ISXS}(\vec{\theta}) = br + \frac{\gamma}{2} r^2 \cos 2(\theta - \theta_\gamma) \quad , \tag{1b}$$

$$\psi_{ISEP}(\vec{\theta}) = br + \gamma br \cos 2(\theta - \theta_\gamma) \quad \text{and} \tag{1c}$$

$$\psi_{ISIS}(\vec{\theta}) = br + b'r' \quad . \tag{1d}$$

where $\vec{\theta}$ is angular position on the sky with respect to the lensing galaxy with polar coordinates r (an angle) and θ, b is the lens strength (also an angle), γ is the dimensionless shear, θ_γ gives the orientation of the shear (measured from W to N, consistent with Kochanek 1991), b' is the strength of a second isothermal sphere and r' is angular distance from this second deflector. The shear at any r' for model ISIS is $\gamma = b'/2r'$. Including the two unknown source positions (β_W and β_N) the first three models have 5 free parameters, while the last model has 6 counting the P.A. and distance d of the group from the lens. Centering the coordinate system on the observed position of the galaxy gives 8 observable quantities, the coordinates of the 4 images.

Parameter values and the source position were obtained by minimizing residuals in the source plane. The observed image positions were projected back into the source plane, as were the position uncertainties (which we took to be equal and circular). The latter produce source plane error ellipses with areas inversely proportional to the magnification which are then used as a metric in minimizing the difference between the model source position and the backward projections of the image positions. We take the uncertainty in the galaxy position to be negligible in all but one model, labelled ISIS+, for which the galaxy coordinates were taken as two additional free parameters.

Results for these fits are given in Table 1. The group strengths and distances for the last two models are $b' = 2''.900$ and $2''.734$ and $d = 14''.7$ and $13''.3$ respectively. The strengths correspond to velocity dispersions for the group of 383 and 372 km/s for $\Omega = 1$. In the ISIS+ model the best position for the lensing galaxy was only 11 mas from the position reported by Kristian *et al.* (1993).

The derived model parameters given in Table 1 are similar to those found by others (e.g. Kochanek 1991; Narasimha and Chitre 1992; Keeton, Kochanek and Seljak 1996) for the same system. The elliptical potential (ISEP) fit least well, and would require an E5 or flatter mass distribution. The double isothermal (ISIS) fit significantly better than the isothermal with external shear (ISXS), even when the position of the “tidal” isothermal was fixed at the flux weighted centroid of the neighboring galaxies (c.f. Young *et al.* 1981) at P.A. -116.4° E of N and $d = 19''.1$. This corresponds to a shear at $\theta_\gamma = 63.6°$ N of W. The goodness of fit, the close positional coincidence, and the plausible value of the group velocity dispersion are strong arguments in favor of the ISIS model. Following Narayan and Bartelmann (1996), time delays τ are given by

$$\tau(\vec{\theta}) = \frac{(1+z_l)}{c}\frac{D_l D_s}{D_{ls}}\left[\frac{1}{2}(\vec{\theta}-\vec{\beta})^2 - \psi(\vec{\theta})\right] \quad , \tag{2}$$

where $\vec{\beta}$ is the source position, the distances D are angular diameter distances, and where the subscripts l and s refer to lens and source, respectively. The left and right hand terms inside the square brackets are, respectively, the geometric and gravitational components of the time delay. Also shown in Table 1 are time delays in days computed for $\Omega = 1$ and

$H_0 = 100$ km/s/Mpc, taking the galaxy redshift to be the same as the group redshift found by Henry and Heasley (1986), $z = 0.304$, and the source redshift to be 1.722. For these values we find

$$\frac{(1+z_l)}{c}\frac{D_l D_s}{D_{ls}} = 30.49 \text{ days arcsec}^{-2}.$$

Models with $(\Omega, \lambda) = (0.1, 0.0)$ predict time delays longer by a factor of 1.074; those with $(\Omega, \lambda) = (0.1, 0.9)$ predict delays longer by 1.038.

Model PMXS predicts longer time delays because the lensing galaxy is more centrally concentrated. Wambsganss and Paczynski (1994) have noted this effect and emphasize the difficulty in constraining the degree of central concentration with only the positions of 4 images. Model ISEP predicts longer time delays because the source must lie near the "diamond caustic" to produce the two brighter images. The diamond caustic for an ISEP model is roughly twice that of an ISXS model with the same shear, forcing the source further off center and increasing the difference in arrival time. A change in position of the lens of 11 mas produces a 3% change in the $B - C$ time delay. Kristian *et al.* (1993) quote a 50 mas uncertainty for that position.

Comparison of the observed $B - C$ delay of 23.7 days with the predictions of Table 1 gives $H_0 = 84$, 44, 64, 41 and 42 km/s/Mpc for the PMXS, ISXS, ISEP, ISIS and ISIS+ models, respectively. The 14% uncertainty in the time delay gives a 14% uncertainty in each of these numbers. Interpolating between the PMXS and ISXS models, we estimate that taking the leading term in equations (1b-d) to vary as $r^{1\pm0.2}$ produces an additional 14% uncertainty in the Hubble constant.

In all of the models the $A - C$ delay is consistently a factor of 1.5 larger than the $B - A$ delay, while the measured $A - C$ delay is a factor of 1.5 *smaller.* While this discrepancy is only at the 2σ level for our adopted uncertainties, it is nonetheless cause for concern. We believe that the $B - C$ delay is less subject to systematic error than either of the shorter delays because of the larger number of samples per time delay.

6. Prospects for Improvement

There are many ways in which our time delay and distance estimate might be improved upon. As described above, the intranight scatter in the photometry is considerably closer to the photon limit than the night-to-night scatter. We expect that a new reduction with improved algorithms, a better profile for the lensing galaxy and perhaps with better flatfielding will improve the scatter and decrease the uncertainty in the time delay. Better algorithms may allow the inclusion of roughly 20 nights of WIYN data which fill many of the gaps and have not been included in the present analysis. Finally, not all of our data have been reduced. Some 25 nights of data taken with the Hiltner telescope, the NOT, and DuPont telescope await reduction. Further monitoring would likewise reduce the uncertainties in the time delays and help to clarify the discrepancy between the observed intermediate delays and those predicted by our models. New HST data to be obtained during Cycle 6 is expected to reduce the uncertainty in the lens position and give an ellipticity for the lensing galaxy.

We thank M. Pierce for obtaining observations of PG1115+080 on our behalf. PLS thanks G. Canalizo and E. Fulton for their early efforts in PSF fitting and lens modelling, and P. Steinhardt for pointing out a small numerical error in an early version of the manuscript. DOR thanks the Institute for Advanced Study for its hospitality.

REFERENCES

Angonin-Willaime, M.-C., Hammer, F. and Rigaut, F., 1993, Gravitational Lenses in the Universe, J. Surdej, D. Fraipont-Caro, E. Gosset, S. Refsdal, and M. Remy, Liege: Institut d'Astrophysique, 85

Blandford, R. D. and Kochanek, C. S., 1987, ApJ, 321, 658

Blandford, R. D. and Narayan, R. 1992, ARA&A, 30, 311

Grogin, N. and Narayan, R., 1996, ApJ, 464, 92

Haarsma, D. B., Hewitt, J. ,N., Lehar, J. and Burke, B. F. 1996a, IAU Symposium 173: Astrophysical Applications of Gravitational Lensing, J. N. Hewitt and C. S. Kochanek, Dordrecht: Kluwer, 43

Haarsma, D. B., Hewitt, J. ,N., Lehar, J. and Burke, B. F. 1996b, preprint, astro-ph/9607080

Henry, J. P. and Heasley, J. N., 1986, Nature, 321, 139

Hogg, D. W. and Blandford, R. D. 1994, MNRAS, 268, 889

Keeton, C. R., Kochanek, C. S., and Seljak, U. 1996, preprint, astro-ph/9610163.

Kochanek, C. 1991, ApJ, 373, 354

Kristian, J., Groth, E. J., Shaya, E. J., Schneider, D. P., and Holtzman, J. A., 1993, AJ, 106, 1330

Kundić, T., *et al.* 1996, preprint, astro-ph/9610162.

Narasimha, D. and Chitre, S. M., 1992, Gravitational Lenses, R. Kayser, T. Schramm and L. Nieser, Berlin: Springer-Verlag, 128

Narayan, R. and Bartelmann, M., 1996, Formation and Structure of the Universe, A. Dekel and J. Ostriker, Cambridge: Cambridge University Press.

Press, W. H., Rybicki, G. B., and Hewitt, J. N., 1992, ApJ, 385, 404

Refsdal, S. 1964, MNRAS, 128, 307

Schechter, P. L. and Moore, C. B., 1993, AJ, 105, 1

Schechter, P. L., 1996, IAU Symposium 173: Astrophysical Applications of Gravitational Lensing, J. N. Hewitt and C. S. Kochanek, Dordrecht: Kluwer, 263

Schild, R. E. and Cholfin, B., 1986 ApJ, 300, 209

Vanderriest, C., Vlerick, G., Lelievre, G., Schneider, J., Sol, H., Horville, D., Renard, L. and Servan, B. 1986, A&A, 158, L5

Weymann, R. J., Latham, D., Angel, J. R. P., Green, R. F., Liebert, J. W., Turnshek, D. E., and Tyson, J. A. 1980, Nature, 285, 641

Witt, H. J., Mao, S. and Schechter, P. L. 1995, ApJ, 443, 18

Young, P. J., Deverill, R. S., Gunn, J. E., Westphal, J. A., and Kristian, J. 1981, ApJ, 244, 723

This preprint was prepared with the AAS LaTeX macros v4.0.

Fig. 1.— An I filter direct image of PG1115+080 showing QSO components $A1, A2, B$, and C. Stars “B” and “C” of Vanderriest *et al.* (1986) are outside the field.

Fig. 2.— Unshifted light curves for the PG1115+080 components components $A1 + A2$ ($\star$), C ($\circ$), and B ($\bullet$) and for reference star “B” ($\Box$).

Fig. 3.— Light curve for component C ($\circ$) shifted by 23.7 days to match that of component B ($\bullet$).

Table 1: Model Parameters and Time Delays for Lens Models

model	b	β_W	β_N	γ	θ_γ	A1-C	A2-A1	B-A2	B-C	χ^2/DOF
	(")	(")	(")	( )	(°)	(d)	(d)	(d)	(d)	
PMXS	1.137	-0.047	0.205	0.198	65.8	12.5	0.13	7.3	19.9	135/3
ISXS	1.144	-0.025	0.108	0.103	65.8	6.6	0.07	3.8	10.4	104/3
ISEP	1.164	-0.022	0.151	0.079	65.7	9.7	0.43	5.0	15.1	204/3
ISIS	1.033	2.598	-1.124	0.099	65.1	5.6	0.06	4.0	9.7	10/2
ISIS+	1.026	2.446	-1.056	0.103	64.9	5.7	0.07	4.2	10.0	0/0

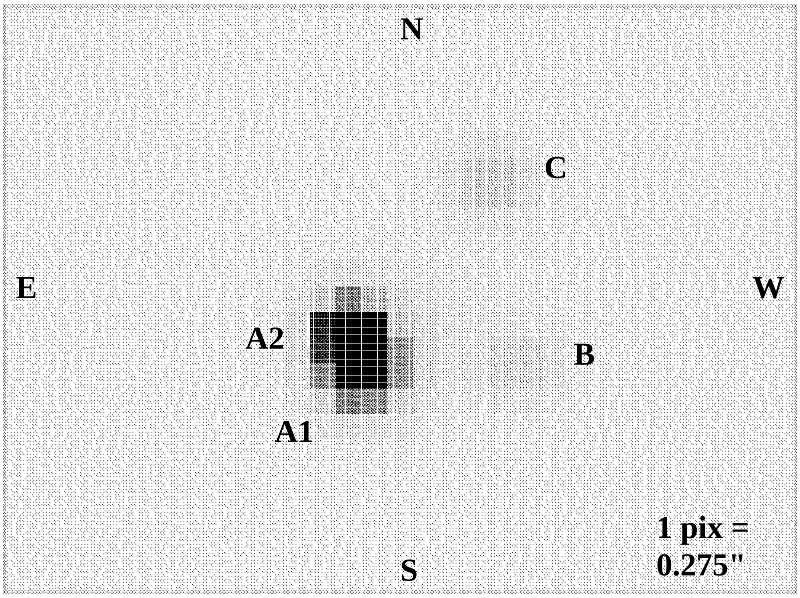
N
C
E
W
A2
B
A1
1 pix =
0.275"
S

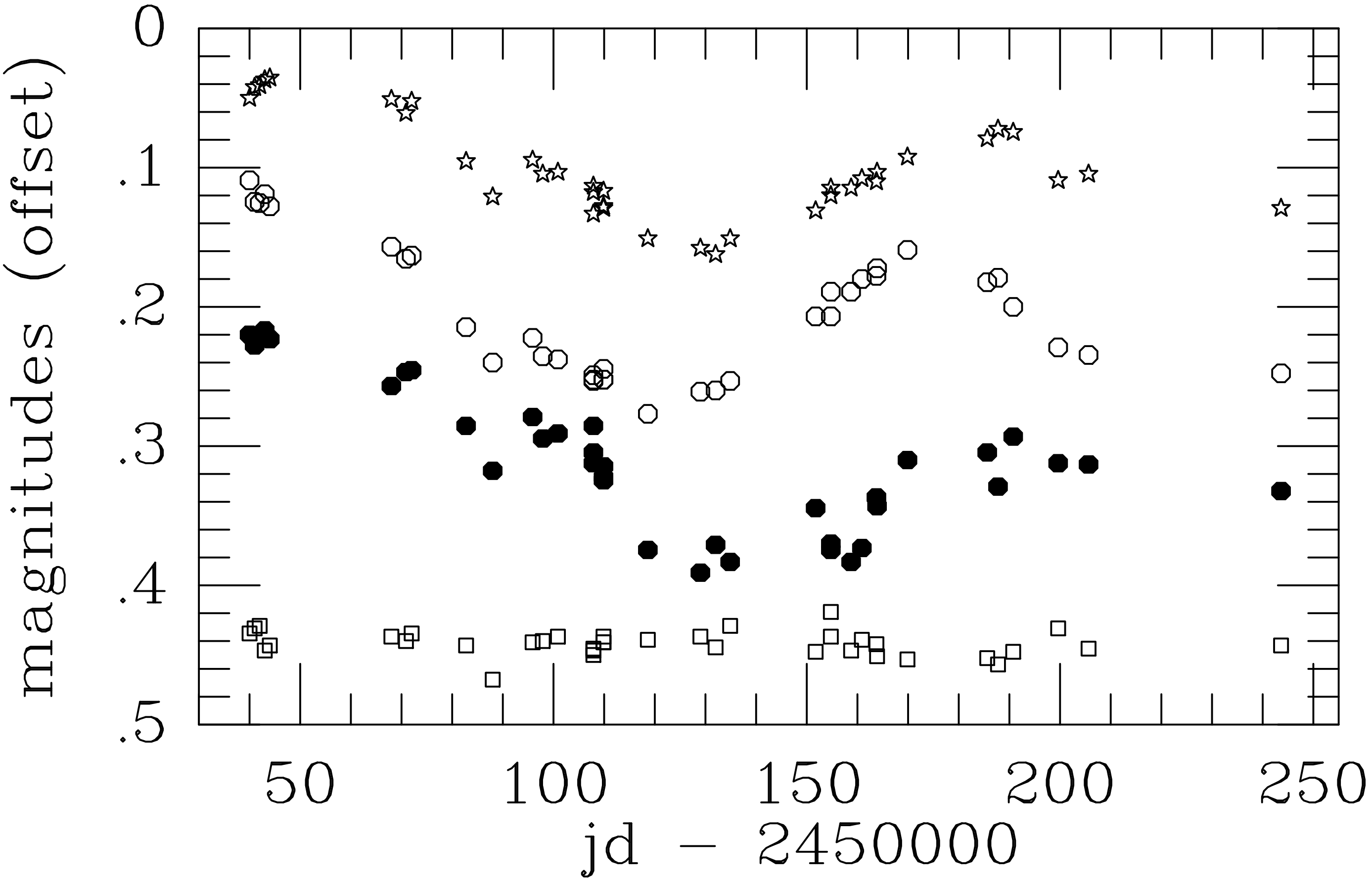
magnitudes (offset)
0
.1
.2
.3
.4
.5
50
100
150
200
250
jd − 2450000

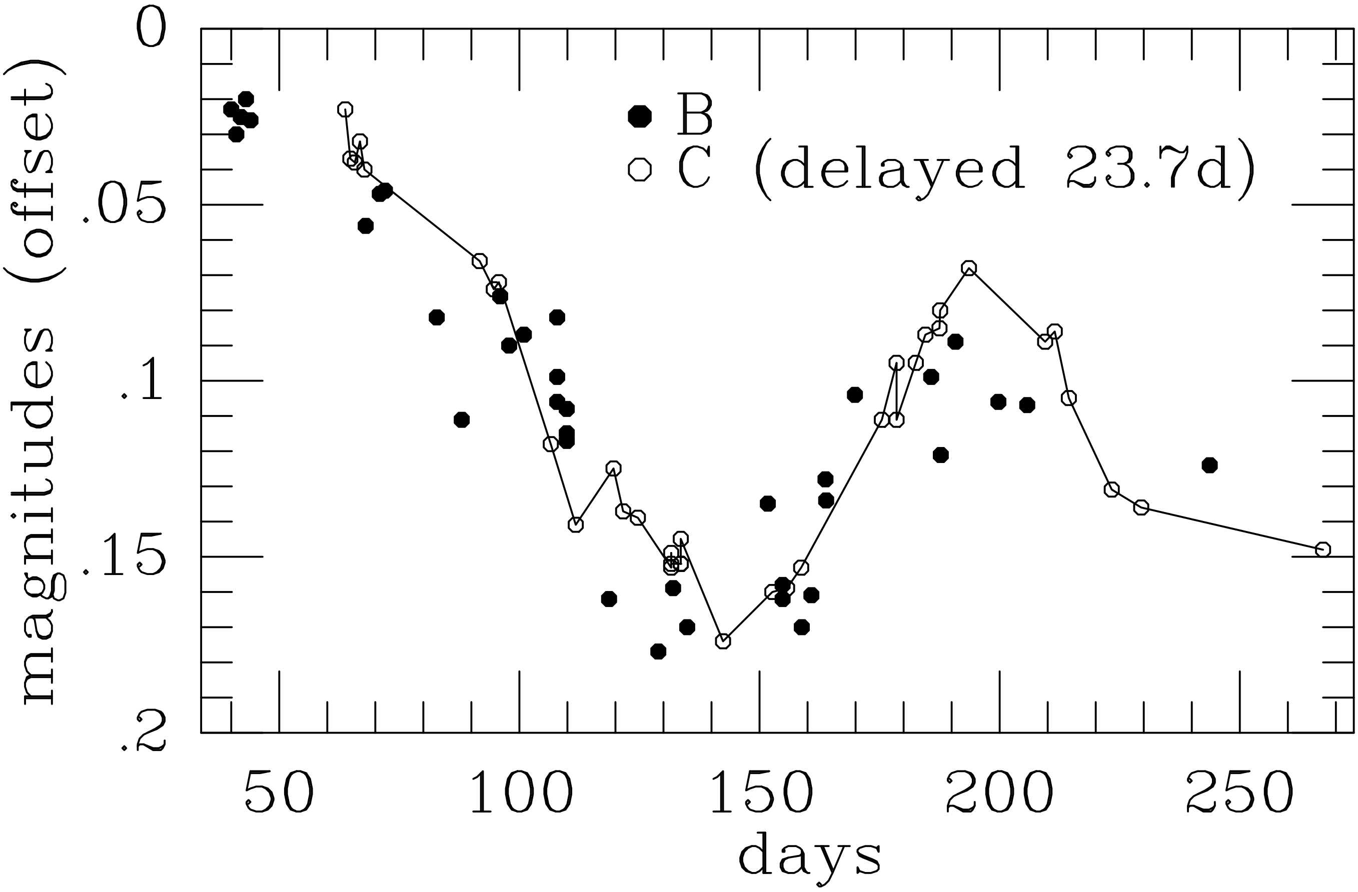
magnitudes (offset)
0
.05
.1
.15
.2
B
C (delayed 23.7d)
50
100
150
200
250
days